Anisotropic scaling of tethered self-avoiding membranes

David Boal, Edward Levinson, Damin Liu, and Michael Plischke
Department of Physics, Simon Fraser University, Burnaby, British Columbia, Canada V5A 1S6
(Received 27 April 1989)

Extensive Monte Carlo simulations are reported of a model for tethered membranes that includes bending rigidity and self-avoidance. These simulations are performed over a range of temperature and for embedding dimensions $d=3$, 4, and 5. The membranes have a stretched configuration that is hexagonal with linear dimension L in the range 5–25. The equilibrium shape of the membranes is analyzed by calculating the eigenvalues of the inertia tensor as well as structure factors $S(k)$ with k in the direction of the eigenvectors of this tensor. The eigenvalues and structure factor show a scaling behavior which indicates that in the thermodynamic limit the membranes are flat rather than crumpled for all temperatures and particle diameters, except possibly in the very weak self-avoidance limit, similar to the "phantom" membrane (one in which particles that are not nearest neighbors on the network do not interact, i.e., they can pass through each other).

I. INTRODUCTION

Random surfaces have received considerable attention over the past several years because of their importance in such systems as microemulsions, biological membranes, and vesicles. There has been a substantial amount of work both of a formal and numerical nature on simplified models of membranes. Of interest in this paper is a particular model of two-dimensional surfaces referred to as the tethered-membrane model, introduced by Kantor, Kardar, and Nelson.[1,2] Among other characteristics, this model has a phase transition, as function of temperature, from a low-temperature flat phase to a high-temperature crumpled phase when the long-range self-avoidance of the surface is neglected.[3,4]

In its simplest form, the model membrane consists of hard spheres connected in a fixed geometry by flexible strings (which join the centers of the spheres, not the surfaces). The form of the membrane that is used in this paper has hexagonal symmetry and its connectivity is illustrated in Fig. 1. The number of vertices along the long direction of the hexagon is denoted by L. To prevent self-intersection of the surfaces, the maximum center-to-center distance l of the strings must be less than $\sqrt{3}\sigma$, where σ is the diameter of the spheres. If l/σ is greater than $\sqrt{3}$, there is still an excluded-volume effect but the membrane is not truly self-avoiding.

Long-range self-avoidance is a computationally intensive feature to incorporate into computer simulations. In the work of Kantor and Nelson on the "phantom" membrane (in which excluded-volume interactions among non-neighboring atoms were not included), self-avoidance was included only at the nearest-neighbor level, and even this was computationally nontrivial. In their calculation,[3,4] it was found that the membrane exhibited a sharp transition between a low-temperature flat phase and a high-temperature crumpled phase. Extensive recent simulations of Ambjorn *et al.*[5] have confirmed this conclusion. Recently,[6] we performed a finite-temperature Monte Carlo simulation in which long-range self-avoidance was explicitly imposed. The model Hamiltonian which we used was slightly different from that of Refs. 3 and 4, although it was equivalent in the limit of small deformations and was chosen in order to increase the speed with which the Monte Carlo simulation could be executed. We found no evidence for the crumpled phase in the case $l/\sigma=\sqrt{3}$ when self-avoidance was taken into account but did find a crumpling transition for the phantom membrane.

In this paper we present the full results of our simulation studies. In Sec. II the model is reviewed and the relaxation times required for the production of uncorrelated Monte Carlo configurations are estimated. As a check on the relaxation mechanism, we perform a set of calculations in which the initialization of the membrane is chosen to be either flat or very highly crumpled. These studies are reported in Sec. II as well.

Section III contains the results of the simulations with long-range self-avoidance, both at finite and infinite tem-

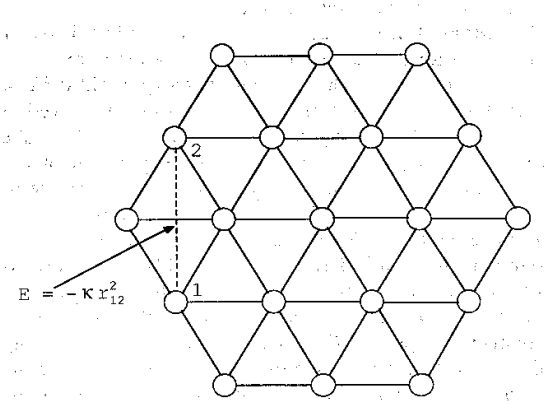

FIG. 1. Planar configuration of a tethered membrane of linear dimension $L=5$. The solid lines represent flexible strings and the dashed line indicates the second-neighbor interaction responsible for the bending rigidity.

perature. Our previous results are extended to larger membrane sizes, up to $L=25$. Our analysis indicates that the phase transition of the phantom membrane is not present in the self-avoiding membrane. Where they can be compared, our numerical results are in agreement with the infinite temperature self-avoiding membrane calculations of Kantor, Kardar, and Nelson,[1,2] although our analysis of the simulations and interpretation of the results are different.

In order to investigate under what conditions the phase transition occurs, we decrease the sphere diameter below $l/\sqrt{3}$ to allow a condition which we refer to as weak self-avoidance. Our results are consistent with the conjecture that there is no crumpled phase for any $\sigma>0$ although it is impossible to rule out the possibility of a crumpling transition for very small diameters. These results are consistent with recent molecular-dynamics simulations of Abraham, Rudge, and Plischke[7] and are summarized in Sec. IV.

We also embed the two-dimensional membrane in four and five dimensions. At infinite temperature we find that the eigenvalues of the inertia tensor grow more slowly with L as the embedding dimension increases. However, we still do not observe the crumpling transition characteristic of the phantom membrane. These results form the material of Sec. V. Finally, our conclusions are summarized in Sec. VI.

II. RELAXATION STUDIES

One of the most important aspects of the Monte Carlo method is ensuring that the sampling procedure has covered a large region of the phase space under consideration. Some systems move through their phase space rather rapidly, while others, for example polymers, move relatively slowly. To investigate the number of time steps (defined in terms of Monte Carlo steps) required for thermalization, we examine the relaxation time of the observables of greatest interest.

The Monte Carlo procedure which we use in this paper is a conventional one: each vertex of the membrane, except the central one which is held fixed to avoid drift of the center-of-mass position of the membrane, is moved in turn. The trial move is chosen randomly within a cube with sides of length $2s$, centered on the position of the vertex. For all of the simulations reported here, the tether length l is taken to be $\sqrt{3}$ and the "stepsize" s is chosen to be 0.2. A Monte Carlo step is defined to be an attempt to move all of the $N=(3L^2+1)/4$ particles except the fixed central particle. The trial move is accepted or rejected according to the conventional procedure of comparing $\exp(-\beta\Delta E)$, where ΔE is the energy difference between the configurations before and after the trial move, with a random number chosen from the interval 0–1. For the relaxation studies, the inverse temperature β is taken to be zero: all moves are allowed unless they violate the hard sphere or tether length constraint. Hence, the results reported in this section are independent of that part of the Hamiltonian associated with the rigidity of the membrane.

For each Monte Carlo step, we calculate the eigenvalues of the inertia tensor I whose matrix elements are given by $I_{jm}=\langle r_j r_m\rangle-\langle r_j\rangle\langle r_m\rangle$, where the angular brackets indicate an average over vertex positions. The smallest and largest eigenvalues are denoted by λ_1 and λ_3, respectively. For a planar membrane, the eigenvector associated with λ_1 is perpendicular to the plane of the membrane, while the eigenvector associated with λ_3 lies in the plane of the membrane. The square of the radius of gyration of the membrane is the trace of the inertia tensor.

For a given observable O of the membrane (the rms radius, for example), we construct the autocorrelation function $C(\Delta t)$,

$$C(\Delta t)=\frac{\langle[O(t+\Delta t)-\langle O\rangle][O(t)-\langle O\rangle]\rangle}{\langle[O(t)-\langle O\rangle]^2\rangle} . \quad (1)$$

In Eq. (1), the angular brackets indicate an average over Monte Carlo steps labeled by the "time" variable t. For each size L of the membrane chosen for study, 10 000 configurations are stored as data points. The number of Monte Carlo steps between stored configurations varies with its size: 10, 20, and 50 steps for $L=5$, 11, and 19, respectively. In order to test the sensitivity of the correlation function to the initialization of the membrane, three different averages are made over the data set by starting the analysis after 1000, 3000, and 5000 configurations.

Typical results for the correlation function associated with one of the eigenvalues of the inertia tensor are shown in Fig. 2 for both the phantom and self-avoiding membranes with $L=19$. The value of the correlation function typically varies by about 0.03 as the starting point of the analysis changes, over the range of time

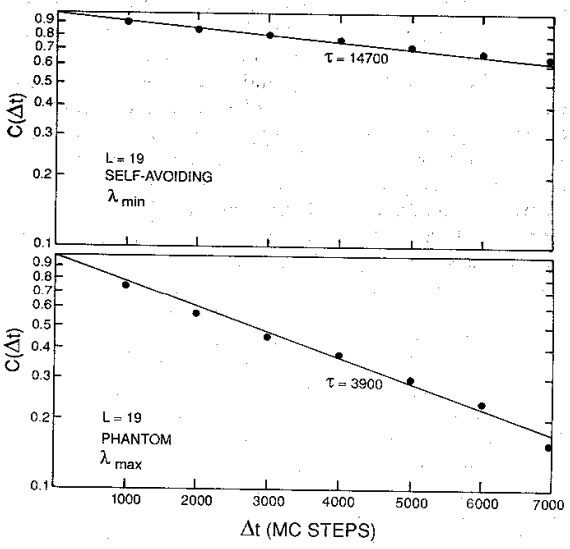

FIG. 2. Correlation function for the smallest eigenvalue λ_1 of the inertia tensor of the self-avoiding membrane (solid curve) and the largest eigenvalue λ_3 of the phantom membrane (dashed curve). Both membranes have dimension $L=19$.

difference shown in the figure. This introduces an uncertainty of about 15% in the estimate of the relaxation time. We assume that $C(\Delta t)\sim\exp(-\Delta t/\tau)$ for small time differences and quote τ as a relaxation time. For the self-avoiding membrane, the longest relaxation times are found for $O=\lambda_1$ and λ_2, while for the phantom membrane the correlations decay most slowly for $O=\lambda_3$. The relaxation time for the rms radius, of course, is dominated by that corresponding to the most correlated eigenvalue. From Fig. 2, one can see that the relaxation time for the $L=19$ self-avoiding membrane is 14 700 Monte Carlo steps, while for the phantom membrane it is 3900 Monte Carlo steps.

In Fig. 3, the L dependence of the relaxation times is shown for both the self-avoiding and the phantom networks. For the self-avoiding network, τ is obtained from the autocorrelation function of λ_1, while for the phantom network, it is determined from that of λ_3. The dependence of the relaxation time on L is consistent with the functional form $\tau\sim L^{3.3}$ for the self-avoiding membrane and $\tau\sim L^2$ for the phantom membrane. These results are in accord with arguments advanced in Refs. 1 and 2. There it is argued that the relaxation time for the phantom network should behave like the Rouse time[8,9] $\tau_R=N/s^2$, where N and s are defined above. The Rouse time is shown for comparison on Fig. 3 as well. In Refs. 1 and 2 it is pointed out that the relaxation time of a self-avoiding membrane should scale as $L^{2+2\nu}$, where ν is the exponent which describes the growth of the rms radius as a function of L. This result is derived under the assumption that there is one diverging length for tethered membranes, namely this rms radius. As we will show later, self-avoiding membranes have two diverging lengths, one of which scales simply as L and one which scales as L^{ν} with $0.65<\nu<0.75$. Our results are therefore consistent with the expression $\tau\sim L^{2+2\nu}$ with the interpretation that ν is the exponent which describes the growth of the width of the membrane.

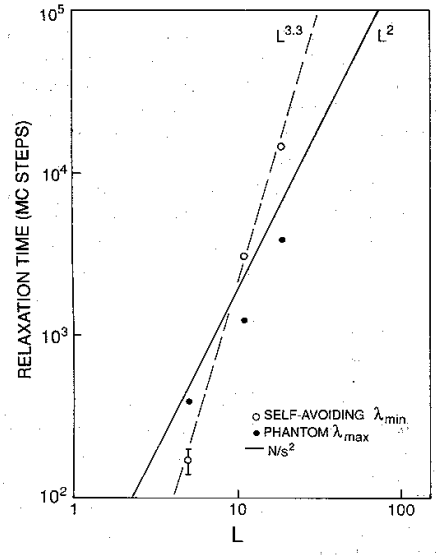

FIG. 3. Size dependence of the relaxation times for the smallest eigenvalue of the self-avoiding membrane and the largest eigenvalue of the phantom membrane. Shown for comparison is the Rouse relaxation time (solid curve).

It is clear from Fig. 3 that for membranes of dimension $L=5$–25 (which is the range of sizes used here) both types of membranes have relaxation times which are of the order of the Rouse time. Hence, we use the Rouse time as the canonical time unit in our studies. Typically, a simulation is run for at least 800 Rouse times to ensure that the phase space of the membrane is adequately sampled. For the largest system, $L=25$, more than 6000 Rouse times are used.

Since part of the purpose of this paper is to study the role of the embedding dimension d, we also evaluate the relaxation time in four and five dimensions. The method used is identical to that used above for three dimensions. It is found that the correlation function decays most slowly for the second largest eigenvalue, although the relaxation time for the largest eigenvalue is typically smaller by less than a factor of 2. The L dependence of the longest relaxation time varies like $L^{3.5\pm0.2}$ for both four and five dimensions. The actual values of the relaxation times at fixed L are very similar for $d=3$–5, although they systematically decrease with increasing d.

The foregoing discussion addresses the short-time relaxation of the tethered membrane. A related concern in our Monte Carlo studies is the possibility that the flat configuration, which we generally take to be the initial state of the membrane, may be in a region of phase space from which the crumpled state cannot be reached—at least in times of the order of Rouse times. To investigate this possibility, we perform a simulation in which a highly crumpled configuration is produced and then used as an initial state for a Monte Carlo simulation.

In order to generate such a highly crumpled configuration, a membrane without bending rigidity (just the infinite temperature case examined above) is subjected to an external Hooke's law potential centered at the center-of-mass position of the network. This potential is turned on slowly and the system is allowed to relax for approximately one Rouse time at each value of the potential strength. The Hooke's law constant is taken to be of the form $\kappa_0 n/\beta$, where $\kappa_0=0.5$, 0.2, and 0.1 for $L=5$, 11, and 19, respectively. The number of the time steps is n, with the length of each time step τ_0 equal to L^2/s^2. For each value of L, 10 simulations are carried out for 15 time steps. It is found that the membrane slowly crumples, as one would expect. Conversely, if the potential is increased too rapidly, the resulting configurations are neither dense nor isotropic in structure: the membrane rapidly becomes locally rigid but does not crumple on a large scale.

First, we check to see if these configurations are, in fact, dense. The rms radius is found to have a dependence on L which scales like $L^{0.69\pm0.03}$ over the range $L=5$–19 for the two-dimensional membrane embedded in three dimensions, and like $L^{0.52\pm0.03}$ over the range $L=5$–9 for the same membrane embedded in four dimen-

sions. Both of these exponents are very near the lower limits set by dense packing arguments, $\frac{2}{3}$ and $\frac{1}{2}$, respectively. The actual numerical values of the rms radii are close to those expected in the dense packing limit. In addition, for the three-dimensional space the asphericity $A=\lambda_1/\lambda_3$ is evaluated as a measure of the anisotropy of the membranes. This number is found to be close to unity for L larger than 10. In contrast, A is found to be much lower when the external potential is absent, as will be shown below.

Having convinced ourselves that the external potential produces highly crumpled and compact configurations, we then turn this potential off and allow the membrane to equilibrate from these crumpled initial configurations. The results of one run with such an initialization are shown in Fig. 4. The behavior of both the rms radius and the asphericity are shown in the figure. One can see that they relax to values typical of a flat configuration within a few Rouse times. Also shown in the figure are averages of these quantities taken over $600\tau_0$ for the flat initializations (the widths are indicated by the error bars). One can see that the characteristics of the highly crumpled membrane rapidly approach those of the flat membrane. In other words, even when the membranes are started off in a part of phase space that may be difficult to access, they move away from that region in a time characterized by the Rouse time for this range of membrane sizes.

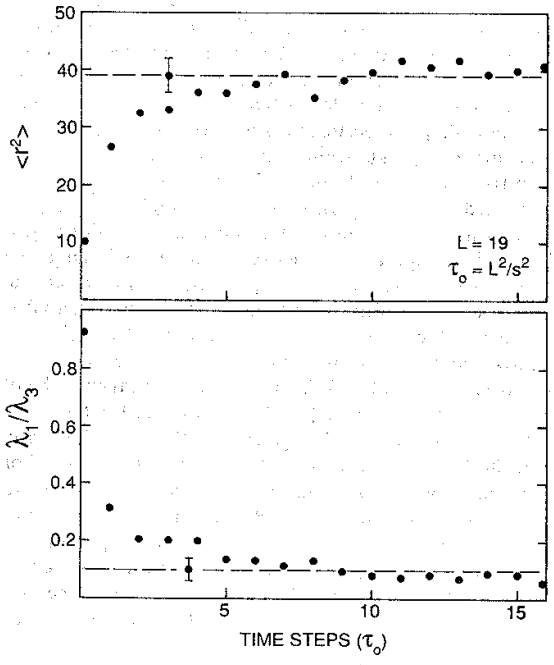

FIG. 4. Time dependence of the rms radius and anisotropy ratio for a highly crumpled initialization. The dashed lines indicate the values for these quantities obtained in an average over $600\tau_0$ with a flat start. The error bars on the dashed line are the widths of the distributions.

III. STRONG SELF-AVOIDANCE

The inclusion of long-range self-avoidance in a simulation is computationally demanding. In its most primitive implementation, a search for the overlap of hard spheres involves an evaluation and comparison of $N^2/2$ distances for each Monte Carlo step. Obviously such a power-law dependence on the self-avoidance algorithm implies that large systems will take prohibitively long to simulate. Since the total number of vertices is proportional to L^2, the overall execution time for the production of independent configurations rises as L^{9-10}: L^2 attempted moves per Monte Carlo step, L^{3-4} for the relaxation time, and L^4 for the self-avoidance check.

In order to obtain results which are applicable to real systems, we wish to simulate as large a membrane as is computationally tractable. Because the execution time rises so rapidly with the size of the membrane, it is necessary to develop algorithms which are both efficient and allow large systems to be investigated. One way of decreasing the time spent on the self-avoidance check is to cover coordinate space with cells whose occupancy is updated continuously. The cells need not be too large if the distance through which a vertex can move within a time step is kept small. Although this procedure adds to the execution time per step, it means that the self-avoidance check scales only as N, or L^2. The procedure chosen here is to make the cells cubic with length equal to the sphere diameter.

A second way of increasing the execution speed is to simplify that part of the Hamiltonian associated with the rigidity of the membrane. In Refs. 1–4, the bending rigidity is modeled by the expression

$$\beta E_b = -\kappa \sum_{i,j} \hat{\mathbf{n}}_i \cdot \hat{\mathbf{n}}_j$$

where the $\hat{\mathbf{n}}$'s are unit vectors normal to the triangular plaquettes defined by the positions of the vertices and where the sum is over nearest-neighbor plaquettes. While inner products of normals appear simple formally, from the computational point of view they are slow, since they involve several multiplications and a division. One can incorporate bending rigidity by means of repulsive springs between second nearest neighbors. This involves no divisions, only the calculation of a distance squared. Our model Hamiltonian for the rigidity is then of the form

$$\beta H = -\kappa \sum_{\{i,j\}} (\mathbf{r}_i - \mathbf{r}_j)^2 , \tag{2}$$

where κ is the bending rigidity and where i and j label second-neighbor pairs on the network. Using this Hamiltonian, and the procedure outlined above for performing the self-avoidance check, we are able to develop a code which allows us to generate statistically significant data sets for membranes up to size $L=25$. In Sec. II it was demonstrated that the relaxation time associated with the size of membrane under consideration here is of the order of the Rouse time, $\tau_R = N/s^2$. Each data set for a given combination of L and κ consists of an initially flat configuration propagated for 800 Rouse times. A total of

20 L-κ combinations are used: $L=5$, 7, 9, and 11 and $\kappa=0.0$, 0.1, 0.2, 0.4, and 1.0. To provide more accurate information on the infinite temperature limit ($\kappa=0$), further simulations are performed at $L=19$ ($2000\tau_R$), $L=25$ ($6000\tau_R$), and the data set for $L=11$ is extended to $1400\tau_R$.

The first quantity of interest which is calculated with this data set is the radius of gyration R_g, or rms radius, of the membrane. We observe that the radii are larger than those of the highly crumpled membranes produced in the external potential examined in Sec. II. Further, the radii are found to grow with κ (increasing rigidity) for fixed L, corresponding to the membrane becoming increasingly flat. Over the range of sizes considered, the rms radii of the self-avoiding membranes scales like L^{ν}. The value of the exponent ν is shown as a function of κ in Fig. 5.

From this figure, one can see that the exponent increases with increasing rigidity: the membrane is flat at large rigidity. However, even at infinite temperature, the rms radius of our membrane grows like $L^{0.93\pm0.03}$. This corresponds to a flatter system than what is obtained in Refs. 1 and 2 for self-avoiding membranes in the shape of a parallelogram (not a hexagon as chosen here), where an exponent of 0.83 ± 0.03 is found. Part of the difference in our results may be attributable to the different shapes of the membranes, and part may arise from the larger membranes used in our simulation. In any event, the exponents which we obtain are significantly larger than the value $\nu=\frac{4}{5}$ predicted by the Flory theory,[1] and much larger than that found for the highly crumpled configurations.

The relatively large value of ν indicates that the membranes may not be particularly crumpled even at infinite temperature. To test this idea, the behavior of the asphericity $A=\langle\lambda_1/\lambda_3\rangle$ is investigated for the $\kappa=0$ configurations. In contrast to the values of A obtained for the highly crumpled membranes of Sec. II, here A is found to be small and to decrease as a function of membrane size: $A(L=5)=0.17$, $A(L=11)=0.12$, $A(L=19)=0.095$, and $A(L=25)=0.088$. Clearly, the membranes are becoming flatter as their size increases.

To obtain further information on the structure of the membrane we calculate the static structure factor

$$S(\mathbf{k})=\frac{1}{N^2}\left\langle \sum_{i,j} e^{i\mathbf{k}\cdot(\mathbf{r}_i-\mathbf{r}_j)} \right\rangle . \tag{3}$$

Since the membranes are not spherical, the structure factor of a particular Monte Carlo configuration is anisotropic and its average will be spherically symmetric only because of the overall rotation of the system. In order to remove the effect of this rotation, we evaluate $S(\mathbf{k})$ for $\mathbf{k}=k\hat{\mathbf{e}}_j$, $j=1,2,3$, where $\hat{\mathbf{e}}_j$ are the eigenvectors corresponding to the eigenvalues λ_j of the inertia tensor $\mathbf{I}$ defined above. The average in (3) thus is taken with respect to the "corotating" frame of reference fixed in the membrane rather than in the "laboratory." This procedure is in contrast to that of Refs. 1–4, where the structure factor is assumed to be isotropic.

The behavior of the structure factors $S(k\hat{\mathbf{e}}_1)$ and $S(k\hat{\mathbf{e}}_3)$ as a function of k is shown in Figs. 6(a) and 6(b). These functions decrease from a value of unity at $k=0$ to a diffractive minimum at $k\approx\pi/\sqrt{\lambda_{1,3}}$. Over this range of k the functions $S(k\hat{\mathbf{e}}_j)$ are well approximated by scaling functions of the form $\phi_j(kL^{\nu_j})$. This is demonstrated in Figs. 6(a) and 6(b) for membrane sizes $L=5$, 11, 19, and 25. For the "perpendicular" structure factor [Fig. 6(a)], corresponding to the smallest eigenvalue of the inertia tensor, $\nu_\perp$ or ν_1 is found to be 0.7, which is the value used in the figure. For the "parallel" structure factor, the exponent which provides the best visual collapse of the data is $\nu_3=\nu_\parallel=0.975$ and we conjecture that in the thermodynamic limit ($L=\infty$) $\nu_\parallel=1.0$. In fact, the form of S_3 is very similar to what one would expect for a disk.

We carry out the same analysis of the structure factors at nonzero temperature and find similar anisotropic scaling behavior. The temperature dependence of the effective exponents $\nu_\perp$ and $\nu_\parallel$ is shown in Fig. 5. The exponent for the perpendicular direction is almost constant at about 0.7, while that for the parallel direction is essentially constant at 1.0. This data support the hypothesis

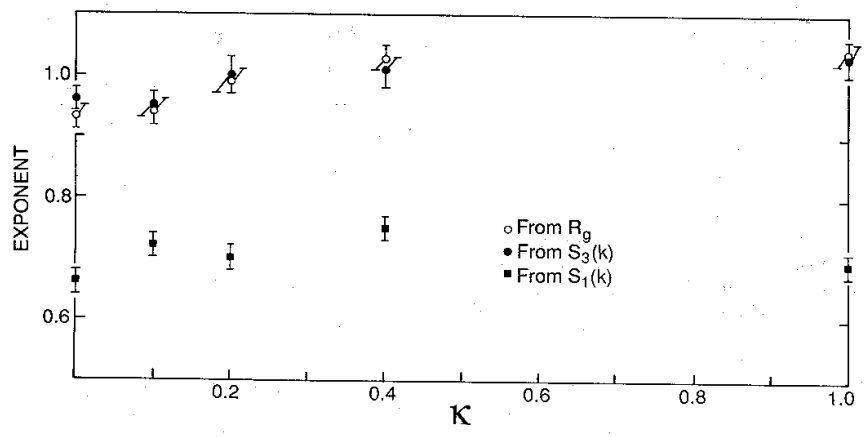

FIG. 5. Temperature dependence of the exponents $\nu_\perp$ and $\nu_\parallel$ for self-avoiding membranes.

advanced above, based on the behavior of the asphericity, that self-avoiding membranes are flat but rough in the sense that the "thickness" given by $\sqrt{\lambda_1}$ does diverge in the thermodynamic limit. Absent here is any indication of a phase transition between an asymptotically flat low-temperature phase and a crumpled high-temperature phase. This is in contrast to the behavior of the phantom membrane[3–5] where such a phase transition is observed.

As a check on our calculations, we repeat the analysis of our data using the methods of Refs. 1–4 and find agreement between the numerical results. That is, if we calculate the spherically averaged structure factor $S(k)$, we find that it is well described by the scaling form $S(k)=\phi(kL^{\nu})$ with an exponent ν roughly equal to 0.8, as expected from the Flory argument. This can, however, be easily reconciled with our results by noting that over most of the scaling region the dominant contribution to $S(k)$ comes from the perpendicular direction $k\hat{\mathbf{e}}_1$ since the diffractive minimum in this direction occurs at much larger values of k than in the other two directions. Thus the effective exponent ν is closer to $\nu_{\perp}$ than to $\nu_{\parallel}$. Further, for our phantom networks, we observe the same phase transition and behavior of the specific heat in the critical region as was found previously.[3,4] However, in examining the temperature dependence of the specific heat in our self-avoiding membranes, we find no evidence of the cusp present in the phantom network. In other words, our numerical work is in agreement with that of Refs. 1–4 where they overlap, but we find no support for the conjecture that there is a crumpling phase transition in strongly self-avoiding tethered membranes.

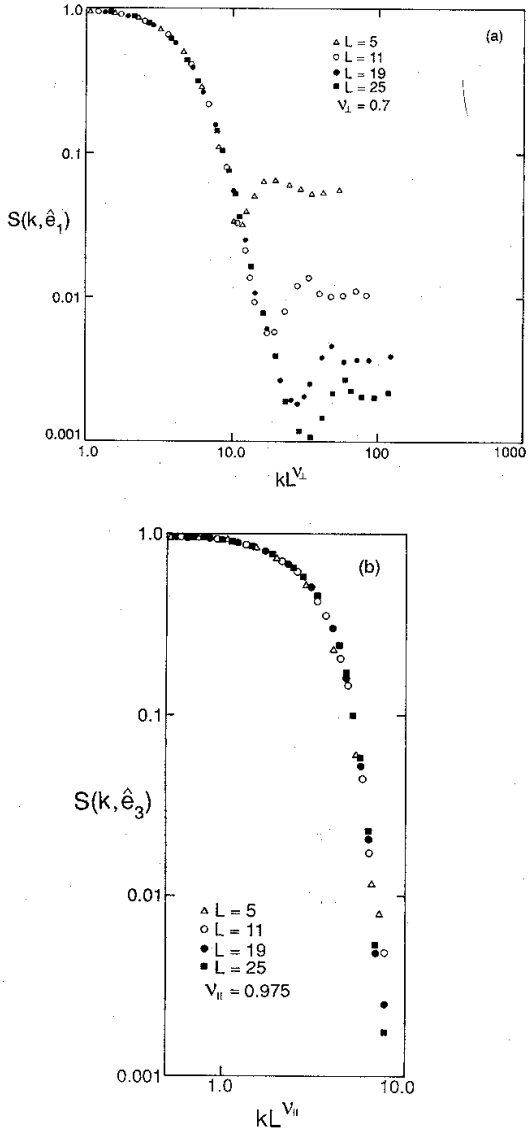

FIG. 6. (a) The "perpendicular" structure factor $S(k\hat{\mathbf{e}}_1)$ for wave vectors in the direction of the eigenvector corresponding to the smallest eigenvalue of the inertia tensor plotted as a function of the scaled variable kL^{ν} with $\nu=0.70$. The structure factors for several values of L are shown: $L=5$ (crosses), $L=11$ (open circles), $L=19$ (solid circles), and $L=25$ (squares). (b) The structure factor $S(k\hat{\mathbf{e}}_3)$ where $\hat{\mathbf{e}}_3$ is the eigenvector corresponding to the largest eigenvalue λ_3 of the inertia tensor. The exponent ν is 0.975 in this case and the symbols have the same meaning as in (a).

IV. WEAK SELF-AVOIDANCE

We have seen, in Sec. III, that strongly self-avoiding membranes are flat rather than crumpled even in the absence of bending rigidity. This result leaves open the possibility that there is a crumpling transition at sufficiently small σ as a function of temperature, or at infinite temperature as function of σ. In order to investigate this possibility, we simulate tethered membranes with a range of values of the parameter σ. The results are displayed in Figs. 7 and 8. For all values of L and σ the data consist

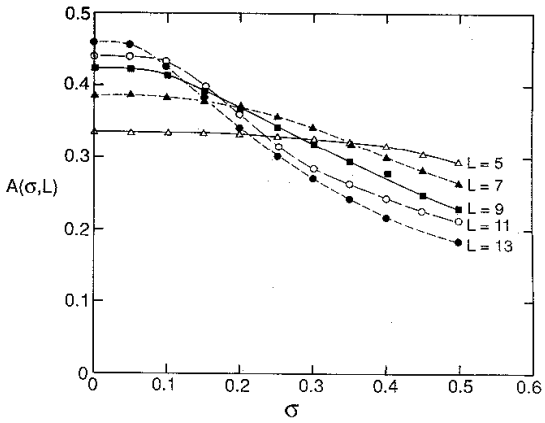

FIG. 7. Behavior of the asphericity A as a function of the sphere diameter σ at infinite temperature for a range of membrane sizes. For small diameters, the membranes are flatter at small L while at larger diameters they are flatter at large L.

of at least 1500 configurations (separated by one Rouse time), and in some cases of 3000 configurations.

In Fig. 7 we plot the asphericity A as function of the hard-sphere diameter σ in the infinite-temperature limit for membranes of size $L=5$, 7, 9, 11, and 13. For small σ, A increases as function of L, as it does in the phantom case ($\sigma=0$). For $\sigma>0.35$, on the other hand, the asphericity decreases monotonically as function of L. This behavior is characteristic of the flat phase. The intersection points of the curves drawn through the data provide a sequence of estimates of the critical diameter σ_c at which the transition from crumpled to flat phase occurs. Examining the data for $L=5$ and $L=9$, we obtain an estimate $\sigma_c(5.9)\approx 0.3$. Similarly, we find $\sigma_c(5,13)\approx 0.2$, $\sigma_c(9,13)\approx 0.14$, $\sigma_c(11,13)\approx 0.09$. We interpret the rapid decrease of σ_c as function of membrane size to mean that *any* $\sigma>0$ is sufficient to destroy the crumpled phase in the thermodynamic limit where L goes to infinity. In this sense, our result is consistent with the well-established result for polymers[8] that σ is a relevant variable (for dimension $d<4$).

Figure 8 displays the same data in a different form. We again plot the asphericity A, this time as function of L for several values of σ. It is seen that for $\sigma\geq 0.1$, the asphericity has a maximum at a value of L less than the maximum (13) that we have used in these calculations. The asphericity for $\sigma=0.05$ is indistinguishable from that of the phantom membrane ($\sigma=0$) for this range of L and for the statistical errors of our calculation. Thus, we can conclude only that self-avoiding membranes are asymptotically flat for $\sigma\leq 0.1$. It must be noted, however, that this is a very small diameter compared to the self-avoiding case ($\sigma=1.0$).

The question of whether or not a crumpled phase exists for very small σ cannot be answered by calculations of this type. As the diameter is decreased, the time required to check for overlap of spheres increases dramatically and, for this reason, our simulations are for smaller membrane sizes than for the strongly self-avoiding case. We are attempting to investigate the possible existence of a crumpling transition by Monte Carlo renormalization-group methods and will report the results of these studies elsewhere.

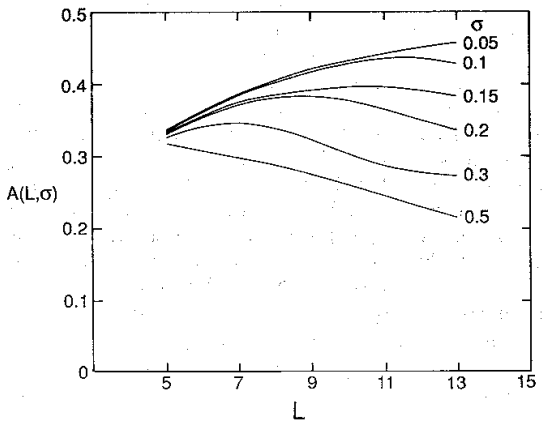

FIG. 8. The asphericity A as function of membrane size L for various σ. For $\sigma\geq 0.1$, the asphericity reaches a maximum value for $L<13$ and decreases, presumably to zero, as L tends to ∞. This figure strongly suggests that for any finite σ, self-avoiding membranes are flat in the thermodynamic limit.

V. STRONG SELF-AVOIDANCE IN FOUR AND FIVE DIMENSIONS

It would appear from the previous two sections that the crumpling transition in three dimensions is limited to conditions in which substantial interpenetration of the membrane is allowed. As the dimensionality of the embedding space is increased, however, there will be significantly more phase space through which the membrane can move and the possibility emerges that the phase transition may reappear even for strongly self-avoiding membranes.

This possibility has been studied by several authors.[10–12] Parisi,[10] in the context of lattice quantum field theory, used a simple random-walk argument to obtain an upper critical dimension $d_{uc}=8$. Subsequent analysis by Gross[11] suggested that random tilings of a torus have $d_{uc}=\infty$. This apparent contradiction was resolved when Cates[12] pointed out that Parisi and Gross considered systems with different connectivity which do not necessarily belong to the same universality class. The systems studied here, like the ones studied by Gross, are of fixed connectivity and have $d_{uc}=\infty$. Thus we do not expect to observe the ideally crumpled phase of the phantom membrane in any finite embedding dimension. However, as we have shown in Sec. IV, self-avoiding membranes have unusual scaling behavior even in the flat phase and it is interesting to examine the dependence on dimensionality of the exponents which characterize the shape.

The main computational difficulty in increasing the embedding dimensionality is the computer memory requirement associated with the self-avoidance check. Using the cell method to keep track of the vertices in a local neighborhood requires a considerable number of cells if they have the same size in each direction. The modification which we make to the method to tame this problem is to change the storage from cubic cells to infinitely long cylinders. The long direction is chosen to be in the direction of the eigenvector belonging to the smallest eigenvalue of the inertia tensor. Because the membrane rotates in coordinate space with time, the long direction is recalculated at least once per Rouse time. This procedure keeps the occupancy of the cells down to a reasonable number of particles.

Machine time limitations restrict the embedding dimensions which we can handle to 5, and L to be no larger than 17. Further, we only examine the infinite-temperature limit since a crumpled phase will appear there, if at all. The method of data analysis is the same as that used in the previous sections: the power-law dependence of the rms radius and of the structure factors on L

TABLE I. Behavior of the exponents ν at infinite temperature in three, four, and five embedding dimensions d. Results are shown for both the rms radii and the structure factors analyzed according to the directions of the eigenvectors associated with the inertia tensor. For the structure factors, the results are given in order of increasing value of the eigenvalue.

	$d=3$	$d=4$	$d=5$
rms radius	0.93	0.79	0.67
Structure factors	0.66	0.62	0.58
	0.99	0.64	0.56
	0.95	0.83	0.57
		0.84	0.72
			0.73

is used as our tool in searching for crumpling.

The results are summarized in Table I for the strongly self-avoiding membrane embedded in three to five dimensions. The exponent for the rms radius is seen to decrease with increasing embedding dimension as one would expect: there is a larger space through which the membrane can move. However, the exponent does not decrease drastically and is substantially above the Flory prediction[1] $\nu(d)=4/(d+2)$ where d is the dimensionality of the embedding space.

The behavior of the structure factors is also summarized in the table. There are, of course, more eigenvectors in the higher dimensions, and the results in the table are ordered from smallest to largest eigenvalue. The inertia tensor shows two large eigenvalues on average, and $d-2$ small ones. Over the range of L which we are able to investigate, the magnitude of the scaling exponents for the largest and smallest eigenvalues decreases with increasing dimension. This is shown graphically in Fig. 9, where a comparison is made between our calculated exponents and the Flory value. The errors shown on the figure are statistical only.

The behavior of the exponents shown in the figure does not mean that the membranes are becoming rougher with increasing dimension. We have also evaluated the asphericity A as a function of L and d. For fixed L, the asphericity shows little dependence on d except for small values of L. However, for all dimensions, A scales as $L^{-2\nu_A}$ with $\nu_A \sim 0.17$, indicating that the membrane is asymptotically flat in $d=3$–5.

VI. CONCLUSIONS

We have performed extensive simulations of the tethered-membrane model with self-avoidance. The relaxation time for the production of uncorrelated configurations is investigated and found to be of the order of the Rouse time for the size of membrane which we could handle computationally. A data set involving at least 400 uncorrelated configurations is generated for each system of interest, by which we mean a membrane characterized by a size, rigidity, strength of self-avoidance, and embedding dimension.

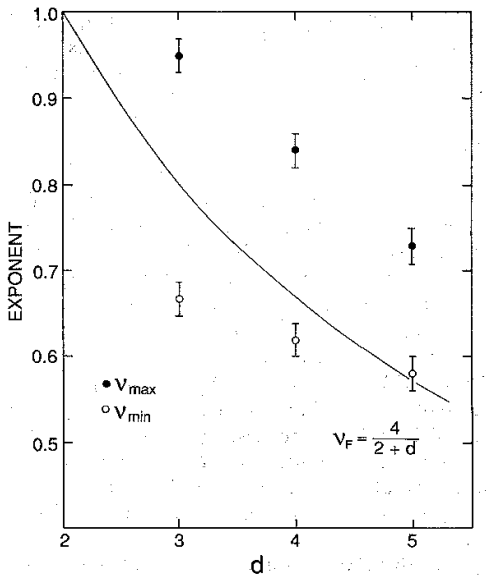

FIG. 9. The largest and smallest of the exponents ν_j in the relation $\lambda_j \sim L^{2\nu_j}$ as a function of embedding dimension d. The Flory exponent $\nu_F=4/(d+2)$ is shown for comparison.

For membranes embedded in three-dimensional space, we find no evidence of a transition between a low-temperature flat phase and a high-temperature crumpled phase: our membranes are observed always to be rough but flat. This is in contrast to the behavior of phantom membranes which are found to possess such a transition.[3–5] The degree to which self-avoidance plays a role is investigated by changing the sphere size compared to the tether length. As the sphere size goes to zero, the membranes become increasingly crumpled, although there is no evidence of a phase transition for any finite σ. This point is under further investigation by Monte Carlo renormalization-group methods.

The membranes are also embedded in higher dimensions to determine whether the transition reappears when the dimensionality of the embedding space becomes large compared to that of the membrane. Machine time limitations restrict our studies to four and five dimensions. We observe the scaling exponents to decrease with increasing dimensionality, insofar as they have been determined from membranes with $L=5$–17. However, the asphericity shows little dependence on the dimensionality, and decreases with L approximately as $L^{-2\nu_A}$ with $\nu_A \approx 0.17$. We conclude that the membranes are asymptotically flat over the range of $d=3$–5.

One of the puzzling aspects of these models is the discrepancy between the results of the calculations reported above and the molecular-dynamics results of Ref. 7 on the one hand and the analytic theories[1,13] (mean-field and renormalization-group) on the other hand. The analytic theories invariably predict a crumpled phase at high enough temperature. The numerical and analytical

results can be reconciled if the hard-core interaction between the particles on the network generates an effective bending rigidity which, for any finite σ is larger than the critical rigidity of the corresponding phantom membrane. This effective rigidity may not appear in the renormalization-group calculations in the low orders to which they have been carried out. While we are unable to demonstrate this analytically, it does not seem to us to be an unrealistic scenario.

ACKNOWLEDGMENTS

The authors wish to thank Farid Abraham, Jim Glosli, Nigel Goldenfeld, Mehran Kardar, David Nelson, Michael Wortis, and Peter Young for useful discussions and Yacov Kantor for helpful correspondence. This work was supported in part by the Natural Sciences and Engineering Research Council of Canada.

[1]Y. Kantor, M. Kardar, and D. R. Nelson, Phys. Rev. Lett. **57**, 791 (1986).
[2]Y. Kantor, M. Kardar, and D. R. Nelson, Phys. Rev. A **35**, 3056 (1987).
[3]Y. Kantor and D. R. Nelson, Phys. Rev. Lett. **58**, 2774 (1987).
[4]Y. Kantor and D. R. Nelson, Phys. Rev. A **36**, 4020 (1987).
[5]J. Ambjorn, B. Durhuus, and T. Jonsson, NORDITA report, 1988 (unpublished).
[6]M. Plischke and D. H. Boal, Phys. Rev. A **38**, 4943 (1988).
[7]F. F. Abraham, W. E. Rudge, and M. Plischke, Phys. Rev. Lett. **62**, 1757 (1989).
[8]P. G. de Gennes, *Scaling Concepts in Polymer Physics* (Cornell University Press, NY, 1979).
[9]P. E. Rouse, J. Chem. Phys. **21**, 1272 (1953).
[10]G. Parisi, Phys. Lett. **81B**, 357 (1979).
[11]D. J. Gross, Phys. Lett. **138B**, 185 (1984).
[12]M. E. Cates, Phys. Lett. **161B**, 363 (1985).
[13]M. Kardar and D. Nelson, Phys. Rev. Lett. **58**, 1289 (1987); **58**, 2280(E) (1987); J. A. Aronowitz and T. C. Lubensky, Europhys. Lett. **4**, 395 (1987); B. Duplantier, Phys. Rev. Lett. **58**, 2733 (1987).